Effects of an estuarine plume-associated bloom on the carbonate system in the lower reaches of the Pearl River estuary and the coastal zone of the northern South China Sea

Minhan Dai [a,*], Weidong Zhai [a], Wei-Jun Cai [b], Julie Callahan [c], Bangqin Huang [a], Shaoling Shang [a], Tao Huang [a], Xiaolin Li [a], Zhongming Lu [a], Weifang Chen [a], Zhaozhang Chen [a]

[a] State Key Laboratory of Marine Environmental Science, Xiamen University, Xiamen 361005, China
[b] Department of Marine Sciences, the University of Georgia, Athens, GA 30602, USA
[c] Environmental, Coastal and Ocean Sciences, University of Massachusetts, Boston, MA 02125, USA

ABSTRACT

We observed a phytoplankton bloom downstream of a large estuarine plume induced by heavy precipitation during a cruise conducted in the Pearl River estuary and the northern South China Sea in May–June 2001. The plume delivered a significant amount of nutrients into the estuary and the adjacent coastal region, and enhanced stratification stimulating a phytoplankton bloom in the region near and offshore of Hong Kong. A several fold increase $(0.2–1.8\,\mu g\,Chl\,L^{-1})$ in biomass (Chl a) was observed during the bloom. During the bloom event, the surface water phytoplankton community structure significantly shifted from a pico-phytoplankton dominated community to one dominated by micro-phytoplankton ($>20\,\mu m$). In addition to increased Chl a, we observed a significant drawdown of pCO$_2$, biological uptake of dissolved inorganic carbon (DIC) and an associated enhancement of dissolved oxygen and pH, demonstrating enhanced photosynthesis during the bloom. During the bloom, we estimated a net DIC drawdown of $100–150\,\mu mol\,kg^{-1}$ and a TAlk increase of $0–50\,\mu mol\,kg^{-1}$. The mean sea–air CO$_2$ flux at the peak of the bloom was estimated to be as high as $\sim-18\,mmol\,m^{-2}\,d^{-1}$. For an average surface water depth of 5 m, a very high apparent biological CO$_2$ consumption rate of $70–110\,mmol\,m^{-2}\,d^{-1}$ was estimated. This value is 2–6 times higher than the estimated air–sea exchange rate.

Crown Copyright © 2008 Published by Elsevier Ltd. All rights reserved.

1. Introduction

Estuarine plumes in coastal sea regions are significantly influenced by land-derived discharge emanating from an estuary (Morris et al., 1995). Although the boundary of any specific estuarine plume is often difficult to define given the highly dynamic nature of estuarine plume systems, an essential characteristic of estuarine plumes may be defined by a significant salinity gradient, albeit a considerably weaker gradient than that prevalent in the contiguous estuary (Morris et al., 1995). Plumes are critical areas of land–ocean interaction, where transformation takes place for the export of sediments, nutrients, and organic material from land to the oceans (Dagg et al., 2004 and references therein).

As a result of the river influence, an estuarine plume may be biogeochemically characterized by the high nutrient discharge associated with the river. In addition, an estuarine plume region is usually located in the lower reaches of an estuary, where turbidity is relatively low and conditions are favorable for phytoplankton growth, resulting in enhanced biological activity (Gastona et al., 2006 and references therein). As a consequence, estuarine plumes are frequently sites of spring and summer phytoplankton blooms. Examples of extensively studied plume systems include the Mississippi and Amazon River plumes (Dagg et al., 2004; Lohrenz et al., 1999; Smith and Demaster, 1996). These numerous studies have been primarily devoted to nutrients, fluxes of organic constituents and phytoplankton within the estuaries and/or their associated plumes and coastal regions (Allen, 1997; Cloern, 1996; Harrison et al., this issue; Lohrenz et al., 1999; Morris et al., 1995; Ringuet and MacKenzie, 2005; Sanders et al., 2001; Yin and Harrison, this issue; Yin et al., 2004). Reports on estuarine plume-associated blooms and the carbonate system response, however, have been limited. The Mississippi River plume is a region where a significant drawdown of dissolved inorganic carbon (DIC) has been observed, due to enhanced biological uptake. In association with the DIC drawdown observations have indicated

a concomitant increase in pH while the total alkalinity (TAlk) was conserved (Lohrenz and Cai, 2006). Similar processes have also been shown in the Scheldt plume (Borges and Frankignoulle, 2002).

During a cruise we conducted in the Pearl River estuary and the northern South China Sea (SCS) in May 2001, we observed a phytoplankton bloom in the estuarine plume that was caused by local heavy precipitation. This estuarine plume discharged a significant amount of nutrients into the outer estuary and the adjacent coastal region. Consequently, a phytoplankton bloom was produced in the region near and offshore Hong Kong. This paper aims to report the biogeochemical responses to this bloom event, in particular, the associated phytoplankton community structure changes and the changes in the carbonate system in the context of ecosystem metabolism. Guo et al. (this issue) examine the seasonality of the carbonate system, with a focus on the area within the estuary mouth.

2. Materials and methods

2.1. Study area

The Pearl River is ranked as the 13th largest river in the world, with a water discharge of $330 \times 10^9 \, m^3 \, yr^{-1}$ (Kot and Hu, 1995). It has a catchment area of $450,000 \, km^2$. The drainage area of the Pearl River has a sub-tropical climate, with a long summer, a short winter, and annual rainfall of 1470 mm. Eighty percent of the river discharge takes place in the wet season, from April to September (PRWRC/PRRCC, 1991).

The Pearl River delta occupies an area of $4000 \, km^2$. It has three major tributaries that merge in the delta region, i.e., West River, North River, and East River. The delta is broadly triangular in shape and is surrounded by highly populated cities, with Guangzhou at its northern apex, Hong Kong in the south-east corner and Zhuhai in the southwest corner.

The Pearl River estuary is subject to intense anthropogenic disturbance as it receives an annual wastewater discharge of recently $\sim 5000 \times 10^6 \, ton \, yr^{-1}$ from upstream cities such as Guangzhou, Foshan, and Dongguan (see the Environmental Status Bulletins of Guangdong Province, China; http://www.gdepb.gov.cn/). Agricultural activities have given rise to increasingly high levels of pollution from fertilizers and pesticides. The use of chemical fertilizers in the region increased by 40% between 1986 and 1989 (Neller and Lam, 1994). While these waste/fertilizer discharges have caused persistent hypoxia in the upper reaches of the estuary (Dai et al., 2006), nutrient-related blooms (harmful or non-harmful) have mainly occurred in the lower reaches of the estuary, as further demonstrated in this paper.

2.2. Sampling and analyses

Sampling was undertaken during a cruise onboard the R/V Yanping II between May 13 and June 3, 2001, along a transect from the Pearl River estuary to the southwest to the Dongsha Island on the shelf of the northern SCS (116°E, 20°N) as a part of the project CARbon Transfer, Transport and Transformation (CAR-TTT) (Fig. 1a). Fig. 1b shows the most intensively investigated area/stations, located around the mouth of the Pearl River estuary off Hong Kong where the phytoplankton bloom occurred.

During the cruise, we started our investigation near Sta. 6A, 6, and 7 between May 14 and May 17, and then moved offshore to Sta. 2 ($\sim$200 m isobath) (May 17–19). During May 24–25, we surveyed mainly the bloom area off Hong Kong by moving offshore again to Sta. 2. The last cruise leg took place on May 29, when we moved back into the Pearl River estuary from Sta. 2.

During the cruise, we performed underway measurements for dissolved oxygen (DO) and CO_2 partial pressure (pCO_2) along the main transect using an underway system previously described (Zhai et al., 2005a, b). The surface temperature and salinity were measured using an SBE-21 Conductivity–Temperature–Depth/
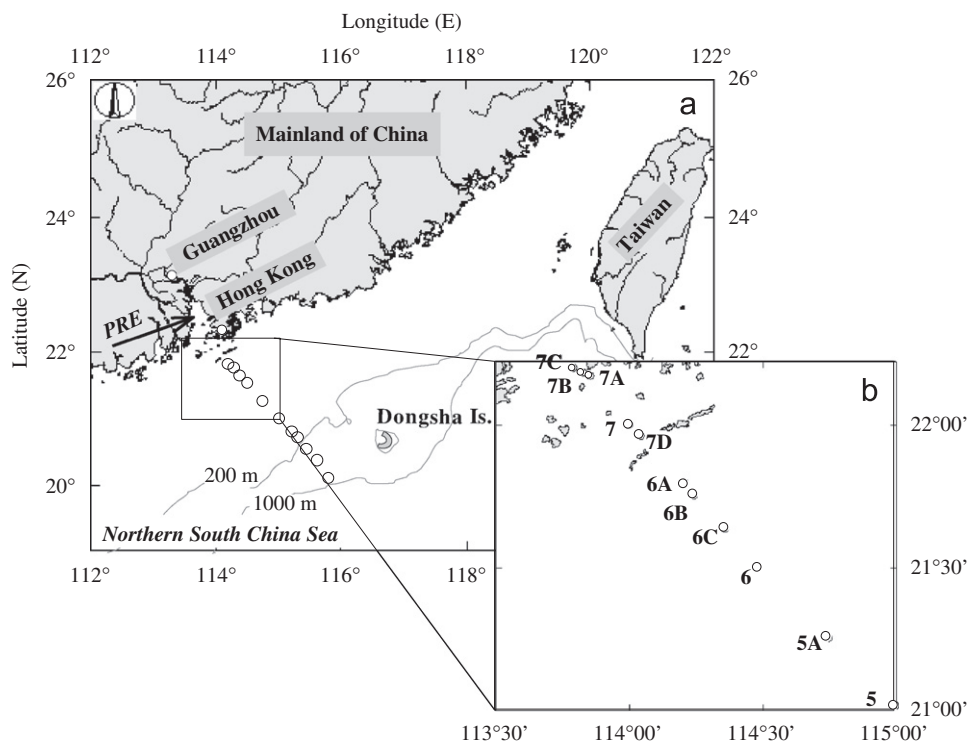

Fig. 1. Maps showing (a) the shelf stations surveyed in May–June 2001 in the northern South China Sea and (b) the sampling stations in the region associated with by the bloom. PRE represents the Pearl River estuary.

Pressure (CTD) unit (Sea-Bird Co.) while vertical profiles of temperature and salinity were determined shipboard with an SBE-19-plus Conductivity–Temperature–Depth/Pressure (CTD) unit (Sea-Bird Co.). Both CTD systems were calibrated in June 2000, as described previously (Cai et al., 2004; Callahan et al., 2004). Together with the SBE-19-plus CTD unit, a rosette sampler fitted with 1.7-L Niskin and/or 2.5-L Go-flo bottles (General Oceanics Co.) was used to take discrete water samples. DO was profiled with a YSI UPS600 meter and was also measured in discrete water samples following the Winkler procedure. Nutrients were determined colorimetrically using a custom-made nutrient analyzer (Tri-223 autoanalyzer) provided by S.C. Pai of the National Taiwan University. All these measurements were made onboard immediately after collecting the samples, as previously described (Cai et al., 2004). The method detection limits are 0.08 μM for nitrite, 0.20 μM for nitrate, 0.17 μM for phosphate, and 0.19 μM for silicate while using 1-cm long cuvette.

DIC data were collected, during and after the cruise (within 2 weeks from sampling) with a Li-Cor® non-dispersive IR detector (Li-6252) after the sample was acidified. This method has a precision of 0.1–0.2% (Cai et al., 2004; Cai and Wang, 1998; Zhai et al., 2005b). TAlk was determined by Gran titration on a 15-mL sample with a Kloehn digital syringe pump, with a precision of 0.1%. Both DIC and TAlk were calibrated against certified reference materials provided by Dr. A. Dickson at the Scripps Institution of Oceanography. pH was measured on discrete samples using a Ross Orion combination electrode. Three NIST traceable pH buffers were used for calibration.

Phytoplankton biomass (Chl *a*) was determined according to standard spectrofluorometric methods (Parsons et al., 1984) using a Hitach 850 fluorometer. The volume of filtration for the analysis depended on the concentration of phytoplankton in the water sample. Typically, 100–150 mL was filtered for estuarine waters and ~1000 mL for offshore waters. Filters were extracted in 90% acetone. In addition, samples were filtered through membrane filters in order to obtain size-fractionated Chl *a*, i.e., pico-phytoplankton (<2 μm), nano-phytoplankton (2–20 μm) and micro-phytoplankton (20–200 μm) (Huang et al., 1999; Wang et al., 1997). Particulate organic carbon (POC) was determined using a CHN analyzer (PE-2400) after carbonate was removed by fuming the filters with concentrated HCl.

3. Results and discussion

3.1. Nutrients associated with the estuarine plume

The Asian Monsoon is one of the major physical forcings affecting the hydrodynamics and biogeochemistry in the SCS and its adjacent waters. The south-western monsoon typically begins in April–May, and is followed by a rainy season. In May 2001, SW winds on May 1, May 6–8, May 13–14, and May 19–22 (Fig. 2a) induced significant precipitation on May 1–4, May 8–9, May 16–18, and May 21–22 (Fig. 2b), recorded at both Baiyun (Guangzhou) (http://ccar.ust.hk) and Hong Kong (http://www.hko.gov.hk) weather observatories. River discharge recorded in the upper river showed a steady increase throughout the month (Fig. 2b).

The accumulated precipitation produced an estuarine plume that was observed in the region off Hong Kong, which can be clearly seen from the transect salinity distribution (Fig. 3). Surface water salinity dropped sharply, from 33–34 to 25–26, at Sta. 6A. The estuarine plume with its low salinity, extended to Sta. 5A. Fig. 3d summarizes the surface salinity distribution against distance, which again shows that the plume dominated a 100 km region between May 23 and 24.
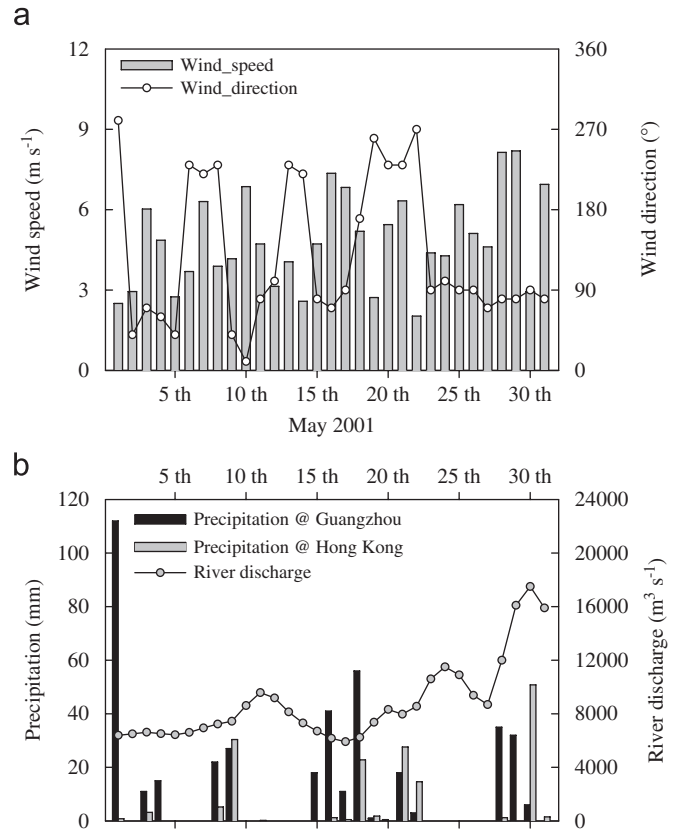

Fig. 2. Daily average of wind speed and direction (a) and precipitation and river discharge (b) in the Pearl River delta in May 2001. Daily river discharge data were from the Pearl River Water Resource Commission.

The rainfall and the associated plume clearly brought a significant amount of nutrients into the region, as demonstrated by an increase in inorganic nitrogen concentrations. At the river end during the survey, high silicate (SiO_3) (~150 μM) and nitrate (NO_3) (75–120 μM) concentrations were observed at levels very similar to those observed in the summer of 2000 (Cai et al., 2004), as well as previous summertime measurements (Zhang et al., 1999). The combination of high river discharge, the increased stratification, and increased nutrient input into the region most likely resulted in the observed relatively high phytoplankton biomass. For instance, total dissolved inorganic nitrogen (DIN) recorded in the surface waters of Sta. 6 during the bloom period (May 24) was almost 10 times higher than values observed during the pre-plume conditions (Fig. 4a). In contrast, phosphate was undetectable or at the level around the lower limit of quantification (2.5–3 times the method detection limit). Silicate did not show significant changes. This should be related to both the biological consumption and the limited input of phosphate.

3.2. Size fractionation structure of phytoplankton during the bloom

During pre-bloom conditions, total Chl *a* was ~0.1–0.2 mg m^{-3} in the both nearshore and offshore surface waters, while a maximum Chl *a* was found offshore at about 90 m (Fig. 5a). During the bloom, however, the nearshore surface Chl *a* reached a maximum level of 1.8 mg m^{-3} (Fig. 5c), an order of magnitude higher than pre-bloom conditions. The vertical profile of this biomass also changed significantly, showing a surface maximum during the bloom in contrast to the subsurface maximum under the pre-bloom condition. Such bloom characteristics disappeared at Sta. 5A (Fig. 5c), where the plume started to decrease (Fig. 3).

Corresponding to the measured increase in phytoplankton biomass, an increase in the particulate organic carbon (POC) concentration was observed in the area of bloom. During the

bloom, POC concentrations in the surface waters of Sta. 6, 6B, and 6C reached 30–40 μmol L^{-1} (Fig. 5d), which was also an order of magnitude higher than the value in the pre-bloom period at Sta. 6 (Fig. 5b). Moreover, the vertical profile of POC at Sta. 6B showed a substantial increase in POC throughout the water column on May 24 (Fig. 5d). No significant variation of the surface POC between pre-bloom and bloom conditions at Sta. 5A was observable (Fig. 5b and d), which again suggests that the bloom signal disappeared at Sta. 5A.

In the bloom region, phytoplankton community structure, in terms of size-fractioned Chl a, significantly shifted from a pico-/nano-phytoplankton-dominated community to one dominated by micro-phytoplankton ($>20\,\mu$m) in the surface water and by the mixture of micro- and pico-phytoplankton in the bloom region in subsurface (Fig. 6).

Under pre-bloom conditions, micro-phytoplankton prevailed at Sta. 7 throughout the water column, while at Sta. 5, an offshore station, micro-phytoplankton were only observable at depth. The size distribution at Sta. 6 reflects a typical phytoplankton composition consisting of micro- as well as pico-phytoplankton. However, during the bloom, clear micro-phytoplankton dominance was found at both Sta. 6B and 6, especially at the surface. At Sta. 5, outside of the bloom, the distribution did not change significantly.

The changes in phytoplanktonic biomass and community structure caused by the bloom were also revealed by the absorption characteristics observed in a parallel study on seawater optics in the region (Wu et al., 2007). Prior to the bloom, the surface phytoplankton absorption ($a_{ph}(675)$) varied from $0.002\,$m^{-1} at Sta. 6 to $0.004\,$m^{-1} at Sta. 5A, and did not show great changes between the inner shelf and the outer shelf/slope. A subsurface maximum in a_{ph} (675) existed throughout the region, as seen for Chl a described above. During the bloom, the horizontal gradient of $a_{ph}(675)$ substantially increased. Within the bloom region, the surface $a_{ph}(675)$ became one order of magnitude higher than beyond the bloom region offshore. A surface maximum as high as $0.050\,$m^{-1} exceeded the previous subsurface maximum.

More significantly, the blue to red ratio (B/R ratio $= a_{ph}(440)/a_{ph}(675)$) on the inner shelf shifted significantly during bloom conditions. Prior to the bloom, the surface B/R ratios, both on the inner shelf and the outer shelf/slope, were greater than 3, which is typical of picoprokaryote communities (Moore et al., 1995). After
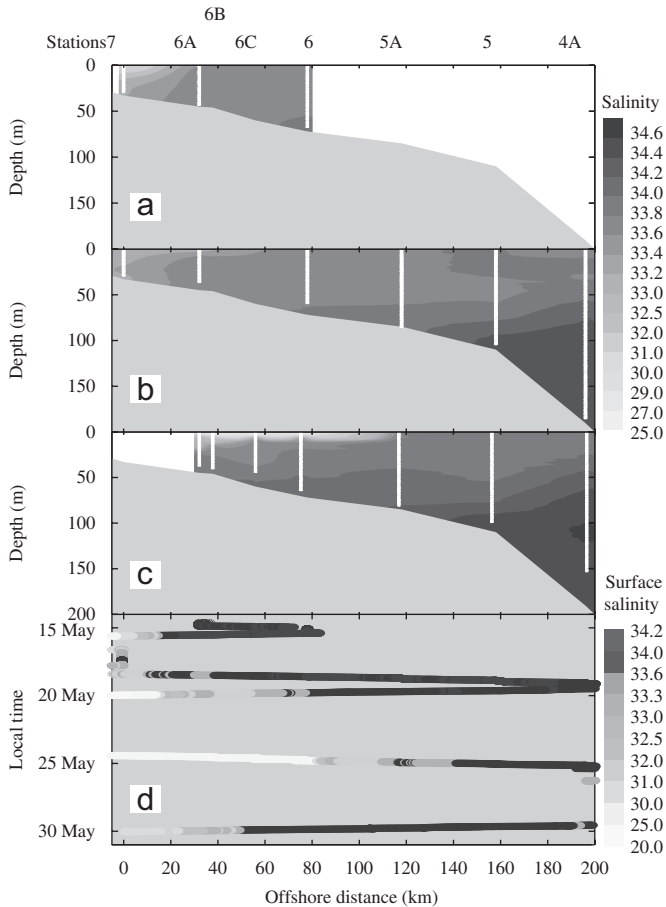

Fig. 3. Comparison of the regional hydrodynamics (vertical profiles of salinity) off Hong Kong under pre-bloom on May 14–16 (a) and on May 17–18 (b), and bloom on May 24–25 (c) conditions. The station sequence from Sta. 7 to 4A reflects the estuarine plume outflow. Also summarized are surface salinity distributions along the survey transect (d).
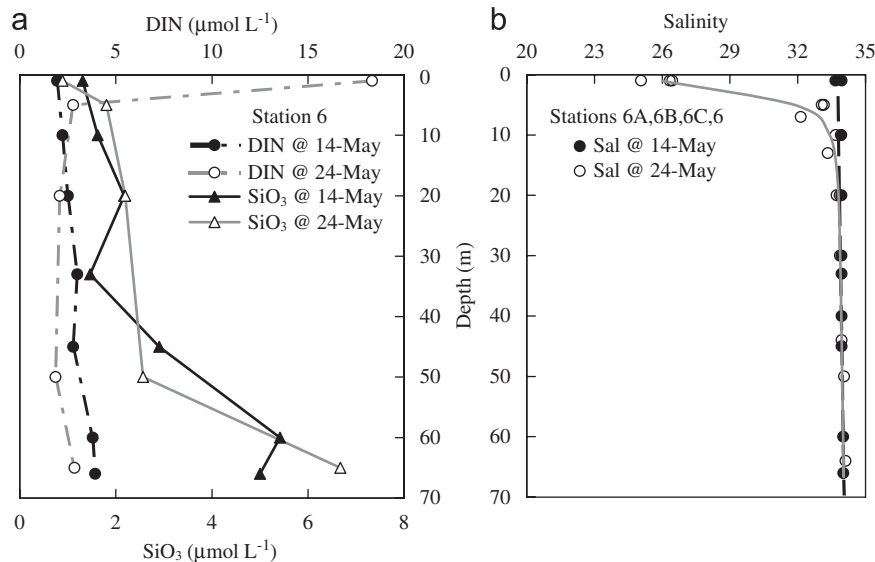

Fig. 4. Vertical profiles of nutrients (a) and salinity (b) at the typical station(s) under pre-bloom/bloom conditions in May 2001 out of the mouth of the Pearl River estuary. DIN/SiO3 refer to the total inorganic nitrogen/silicate.
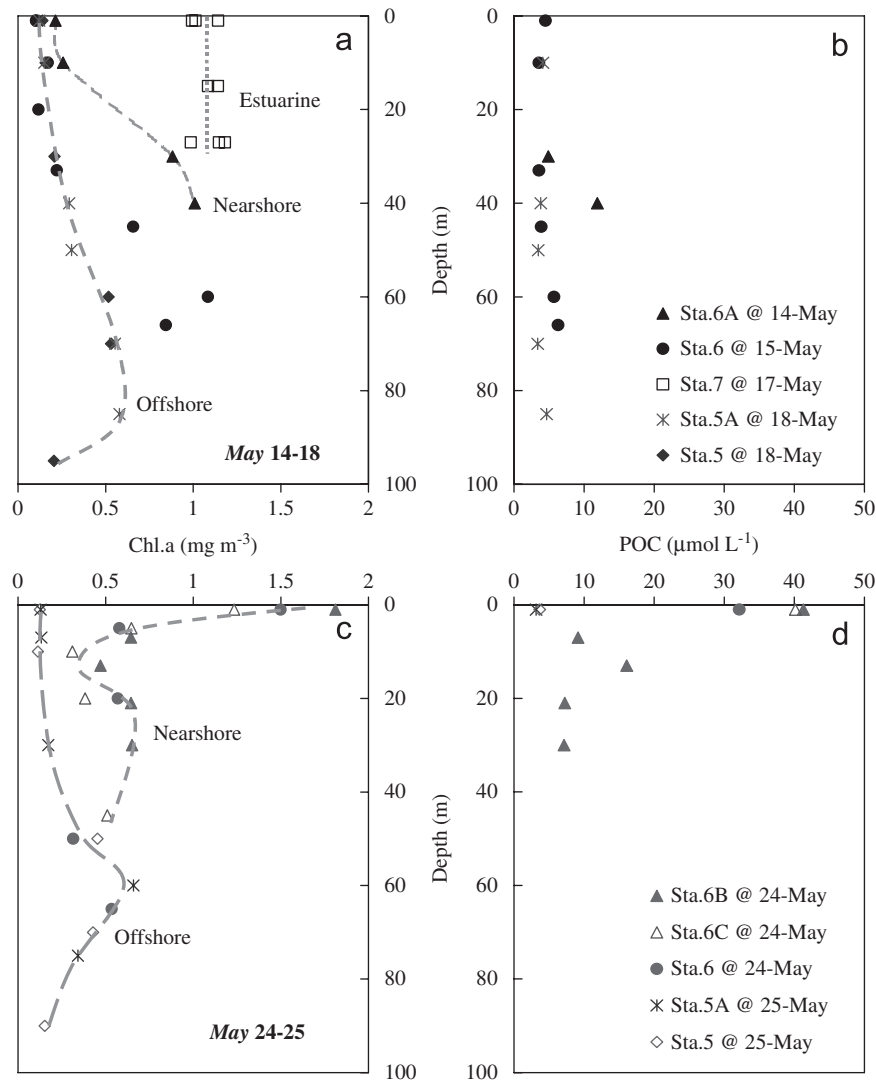
Fig. 5. Vertical profiles of Chl a (a) and particulate organic carbon (b) at several stations during the pre-bloom conditions (May 14–18) as compared to the bloom during May 24–25 (c, d). Salinity profiles were shown in Figs. 3 and 4.

the bloom, B/R ratio at Sta. 6 dropped from 3.9 to 2.5. Strong absorption occurred at 636, 485, and 410 nm, suggesting the dominance of diatoms in the phytoplankton community, since diatoms have absorption peaks at ∼636 and ∼490 nm due to their Chl c and fucoxanthin accessory pigment content (Bidigare et al., 1990). The absorption maxima in the blue region shifted from 440 to 432 and 410 nm, which is indicative of an increasing level of phaeopigments (Lorenzen and Downs, 1986). Outside the bloom region, however, B/R ratios of >3 persisted, even after the bloom. Although the algal species in this bloom were not directly identified, evidence from the absorption data suggests that the community is most likely composed of large-sized or chain-forming diatom species.

3.3. pCO_2 and air–sea CO_2 fluxes during the bloom

As a result of the bloom, we observed significant drawdown of surface water pCO_2 and an increase in DO (Fig. 7). Atmospheric pCO_2 held steady at ∼370 μatm throughout the survey. Under typical biogeochemical conditions, surface water CO_2 is for the most part in equilibrium with the atmosphere in offshore regions in the Spring (Zhai et al., 2005a). This equilibrium condition was

observed on May 14 (∼350 μatm). However, during the bloom, pCO_2 in surface waters dropped to as low as ∼200 μatm. In the follow-up survey on May 29, this pCO_2 decrease became much less pronounced and was restricted to a more confined region. Along with this pCO_2 drawdown, a significant increase in dissolved oxygen was also recorded (Fig. 7b), demonstrating enhanced photosynthesis during the bloom.

The bloom event was accompanied by significant CO_2 uptake. Using the wind speed-dependent CO_2 gas transfer coefficient of Wanninkhof (1992), the estimated sea–air CO_2 fluxes of the bloom area ranged from −23.5 to −15.9 mmol m^{-2} d^{-1} on May 24, and from −15.6 to 3.43 mmol m^{-2} d^{-1} on May 29. Assuming that the bloom reached its maximum on May 24, extending ∼100 km and covering an area of ∼3000 km^2 (since the breadth of the estuary mouth is ∼30 km), the mean sea–air CO_2 flux at the peak of the bloom was about −18 mmol m^{-2} d^{-1}. The mean flux was still about −4.0 mmol m^{-2} d^{-1} 5 days later.

3.4. Response of the carbonate system to the bloom

Another striking biogeochemical response to this bloom, however, was the consumption of inorganic carbon. Along with
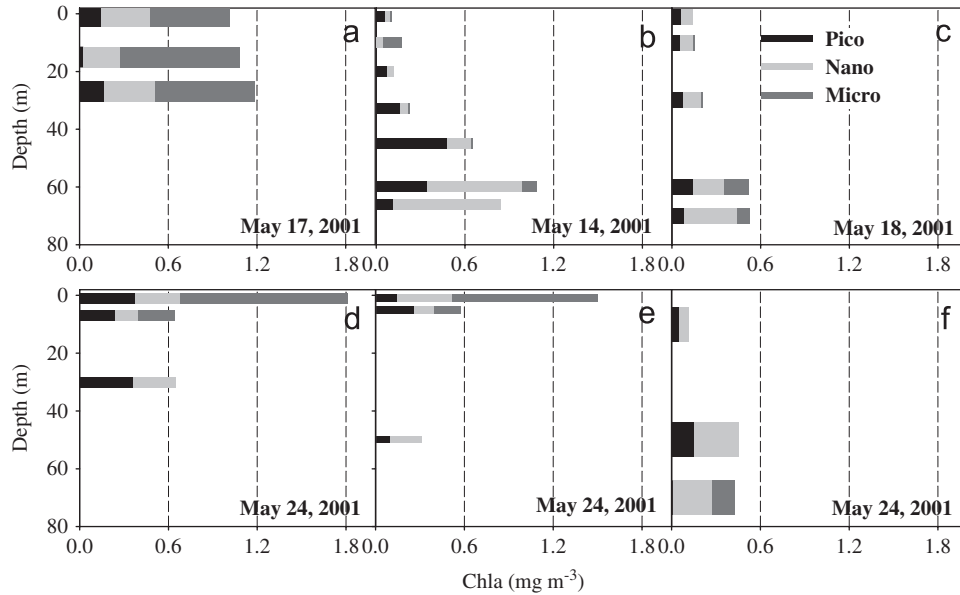
Fig. 6. Size fractionated Chl a ($mg\,m^{-3}$) in the regions associated with the bloom, suggesting the community structure changes during pre-bloom (May 14–18; (a–c)) and bloom conditions (May 24; (d–f)). Note that "pico", "nano", and "micro" represent pico-phytoplankton ($<2\,\mu m$), nano-phytoplankton (2–$20\,\mu m$), and micro-phytoplankton (20–$200\,\mu m$), respectively.
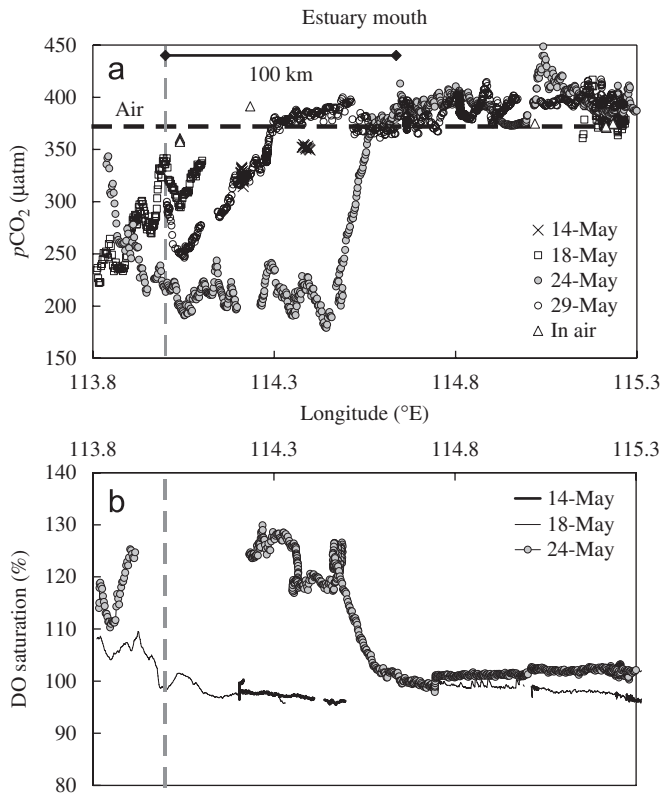

Fig. 7. Surface pCO_2 (a) and dissolved oxygen (b) variations off Hong Kong before (May 14–18) and after (May 24) the bloom.

this bloom event, we observed a significant decrease in surface water DIC (Fig. 8a) and an associated enhancement of pH (Fig. 8b).

During the bloom period, surface pH increased from $\sim$8.2 to as high as $\sim$8.6 (Fig. 8b), due to the removal of protons during photosynthesis. In addition, both DIC and TAlk were significantly lower in the top 5 m of the water column, while DIC was somewhat lower at 10–20 m depth (Fig. 8a).

In order to subtract the influence of water mixing, we plotted DIC vs. TAlk. Since DIC and TAlk behave similarly during water mixing, the DIC-TAlk plot should be a straight-line during simple water mixing. However, if significant photosynthesis/respiration occurs, every unit of Redfield-like organic matter produced or respired during photosynthesis/respiration is associated with 106 units of DIC change, but only a few units of total alkalinity change (i.e. $\Delta DIC/\Delta TAlk \approx -106/17$). Therefore, the DIC-TAlk plot should depart from the non-bloom line during bloom conditions.

At most stations, DIC was significantly linearly correlated with TAlk (Fig. 9a), as was observed in July 2000 (replotted using data from Cai et al., 2004). Major departures from the mixing line towards lower DIC values, suggesting biological uptake, were observed at Sta. 7A, 7B, 7C (near Hong Kong) during the May 17 survey, Sta. 6B, 6C, 6 (on the shelf) during the May 24 survey and Sta. 7D during the May 30–31 survey. However, plots at Sta. 6A (off the estuary mouth) and Sta. 7 (near the estuary mouth) during May 14–17 surveys were located on the non-bloom mixing line (Fig. 9a), which suggests that the "bloom" occurred around May 17 and firstly was geographically limited to inside the estuary mouth. Seven days later, the bloom expanded into the neighboring shelf area.

Fig. 9b portrays the changes in the carbonate system associated with the bloom event. During a typical (non-bloom) flood period in May 2001, the Pearl River estuary and the adjacent northern SCS are characterized by water mixing among three end-members, i.e. the river end-member (DIC $\sim$970 $\mu mol\,kg^{-1}$ and TAlk $\sim$740 $\mu mol\,kg^{-1}$), the surface northern SCS end-member (DIC 1830–1960 $\mu mol\,kg^{-1}$ and TAlk 2240–2340 $\mu mol\,kg^{-1}$) and the deep northern SCS end-member (DIC $\sim$2260 $\mu mol\,kg^{-1}$ and TAlk $\sim$2380 $\mu mol\,kg^{-1}$, located at 500–750 m around the northern slope). The two SCS end-members were also observed during the July 2000 survey, while the river end-member appeared slightly different from the July 2000 (Fig. 9a).

More significantly than the scattering in non-bloom periods, however the fourth end-member, indicative of blooms can be identified based on the DIC-TAlk plots. During the May 17 survey, this bloom end-member (salinity $\sim$25.3, pH $\sim$8.34, DIC $\sim$1660 $\mu mol\,kg^{-1}$ and TAlk $\sim$2030 $\mu mol\,kg^{-1}$) was located in the surface water of Sta. 7A, while it moved to the offshore area around Sta.
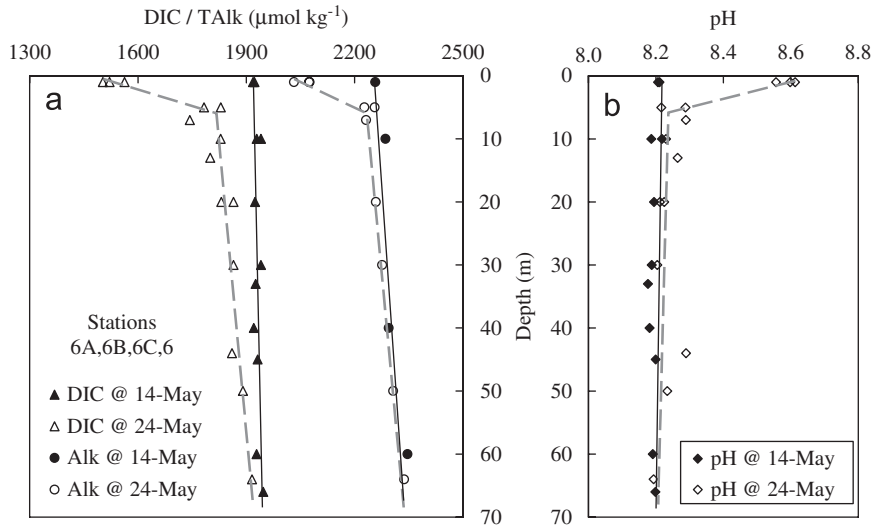
Fig. 8. pH/DIC/TAlk variations in the nearshore shelf waters before (May 14–18) and after (May 24) the bloom under study.
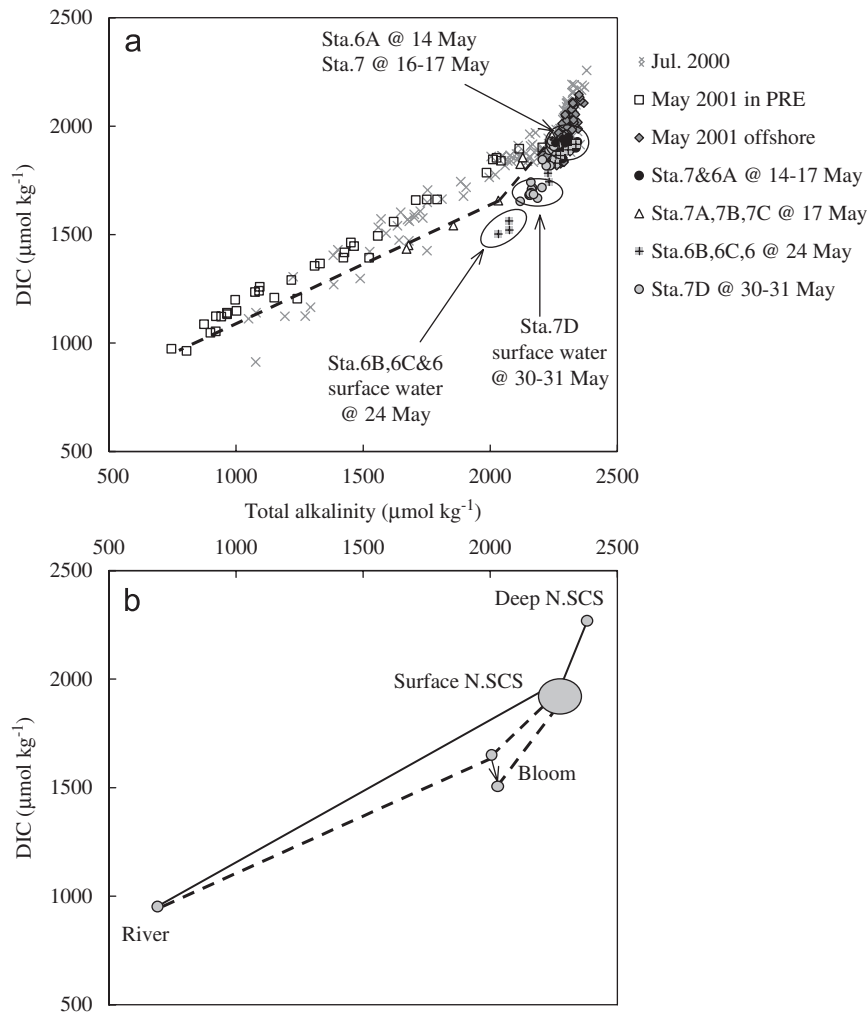

Fig. 9. DIC vs. TAlk (a) and an end-member sketch for the water mixing (b) in the Pearl River estuary and the adjacent northern South China Sea. The July 2000 data shown in (a) were re-plotted using data reported in Cai et al. (2004), while the white squares in (a) were replotted from Guo et al. (this issue) to show data in the Pearl River estuary collected during another leg of the same cruise as this study. In (b), the solid lines show general water mixing lines, while the broken lines show water mixing during different bloom periods. The arrow in (b) shows the direction of evolution of the bloom end-member under study and its approximate quantity.

6B, 6C, and 6 (salinity ~25.1–26.4, pH ~8.55–8.61, DIC ~1500–1560 $\mu mol\,kg^{-1}$ and TAlk ~2030–2080 $\mu mol\,kg^{-1}$ in the surface water) 7 days later. Therefore, during these 7 days, we estimate a net DIC drawdown of 100–150 $\mu mol\,kg^{-1}$ and a TAlk increase of 0–50 $\mu mol\,kg^{-1}$ for the bloom end-member (Fig. 9). For an average surface water depth of 5 m (Figs. 4b and 8), a very high apparent biological CO_2 consumption rate of 70–110 $mmol\,m^{-2}$ d^{-1} was estimated. This value is 2–6 times higher than the estimated air–sea CO_2 exchange rate as referred to above, but would be consistent with a substantial bloom event, as recorded during the survey period.

4. Concluding remarks

Land-derived nutrients have significant impacts on the coastal environment. The case presented here demonstrates the extent to which the coastal environment can be affected by land-based input. Such events may be episodic and short-lived, and therefore specially designed, well-timed experiments are required to investigate events of this nature. It is important to note that the approximate time scale of the bloom event observed in this study was <1–2 weeks, which was, to a large extent, dependent upon the amount of nutrients in the plume. The bloom investigated in this study demonstrates the clear link between estuarine plumes and associated nutrient discharge and enhanced phytoplankton production. Profound biogeochemical responses to such blooms can be assessed through observed changes in the carbonate system.

Finally, we recommend that quantitative assessment of CO_2 fluxes in such episodic but intense events must be taken into account for a better constraint of the air–sea CO_2 fluxes, both at regional and global scales. Although the bloom event that we observed may not supersede the overall source/sink terms of the entire region, more detailed study of such events is needed to determine the relative importance of such events to regional carbon budgets.

Acknowledgements

References

Allen, J.I., 1997. A modeling study of ecosystem dynamics and nutrient cycling in the Humber plume, UK. Journal of Sea Research 38, 333–359.

Bidigare, R.R., Ondrusek, M.E., Morrow, J.H., Kiefer, D.A., 1990. In vivo absorption properties of algal pigments. SPIE Ocean Optics 1302, 290–302.

Borges, A.V., Frankignoulle, M., 2002. Distribution and air–water exchange of carbon dioxide in the Scheldt plume off the Belgian coast. Biogeochemistry 59, 41–67.

Cai, W.J., Wang, Y., 1998. The chemistry, fluxes, and sources of carbon dioxide in the estuarine waters of the Satilla and Altamaha Rivers, Georgia. Limnology and Oceanography 43, 657–668.

Cai, W.J., Dai, M.H., Wang, Y.C., Zhai, W.D., Huang, T., Chen, S.T., Zhang, F., Chen, Z.Z., Wang, Z.H., 2004. The biogeochemistry of inorganic carbon and nutrients in the Pearl River estuary and the adjacent Northern South China Sea. Continental Shelf Research 24, 1301–1319.

Callahan, J., Dai, M.H., Chen, R.F., Li, X.L., Lu, Z.M., Huang, W., 2004. Distribution of dissolved organic matter in the Pearl River Estuary, China. Marine Chemistry 89, 211–224.

Cloern, J.E., 1996. Phytoplankton bloom dynamics in coastal ecosystems: a review with some general lessons from sustained investigation of San Francisco Bay, California. Reviews of Geophysics 34, 127–168.

Dagg, M., Benner, R., Lohrenz, S., Lawrence, D., 2004. Transformation of dissolved and particulate materials on continental shelves influenced by large rivers: plume processes. Continental Shelf Research 24, 833–858.

Dai, M., Guo, X., Zhai, W., Yuan, L., Wang, B., Wang, L., Cai, P., Tang, T., Cai, W.-J., 2006. Oxygen depletion in the upper reach of the Pearl River estuary during a winter drought. Marine Chemistry 102, 159–169.

Gastona, T.F., Schlachera, T.A., Connollyb, R.M., 2006. Flood discharges of a small river into open coastal waters: Plume traits and material fate. Estuarine, Coastal and Shelf Science 69, 4–9.

Guo, X., Cai, W.-J., Zhai, W., Dai, M., Wang, Y., Chen, B., this issue. Seasonal variations in the inorganic carbon system in the Pearl River (Zhujiang) estuary. Continental Shelf Research, in press, doi:10.1016/j.csr.2007.07.011.

Harrison, P.J., Yin, K., Lee, J.H.W., Gan, J., Liu, H., this issue. Physical–biological coupling in the Pearl River estuary. Continental Shelf Research, doi:10.1016/j.csr.2007.02.011.

Huang, B.Q., Hong, H.S., Wang, H.L., 1999. Size-fractionated primary productivity and the phytoplankton-bacteria relationship in the Taiwan Strait. Marine Ecology Progress Series 183, 29–38.

Kot, S.C., Hu, S.L., 1995. Water flows and sediment transport in Pearl River Estuary and waves in South China near Hong Kong. In: Proceedings of a Symposium on the Hydraulics of Hong Kong Waters. Civil Engineering Department, Hong Kong University, pp. 13–32.

Lohrenz, S.E., Cai, W.-J., 2006. Satellite ocean color assessment of air–sea fluxes of CO_2 in a river-dominated coastal margin. Geophysical Research Letters 33, L01601, doi:10.1029/2005GL023942.

Lohrenz, S.E., Fahnenstiel, G.L., Redalje, D.G., Lang, G.A., Dagg, M.J., Whitledge, T.E., Dortch, Q., 1999. Nutrients, irradiance, and mixing as factors regulating primary production in coastal waters impacted by the Mississippi River plume. Continental Shelf Research 19, 1113–1141.

Lorenzen, C.J., Downs, J.N., 1986. The specific absorption coefficients of chlorophyllide *a* and pheophorbide *a* in 90% acetone, and comments on the fluorometric determination of chlorophyll and pheopigments. Limnology and Oceanography 31, 449–452.

Moore, L.R., Goericke, R., Chisholm, S.W., 1995. Comparative physiology of Synechococcus and Prochlorococcus: influence of light and temperature on growth, pigments, fluorescence and absorptive properties. Marine Ecology Progress Series 116, 259–275.

Morris, A.W., Allen, J.I., Howland, R.J.M., Wood, R.G., 1995. The estuary plume zone-source or sink for land-derived nutrient discharges. Estuarine Coastal and Shelf Science 40, 387–402.

Neller, R.J., Lam, K.C., 1994. The environment. In: Yeung, Y.M., Chu, D.K.Y. (Eds.), Guangdong: Survey of a Province Undergoing Rapid Change. The Chinese University of Hong Kong Press, Hong Kong, pp. 23–35.

Parsons, T., Maita, Y., Lalli, C., 1984. A Manual of Chemical and Biological Methods for Seawater Analysis. Pergamon Press, New York, 173 pp.

PRWRC/PRRCC, 1991. The Pearl River Records (Zhujiang Zhi) 1. Guangdong Science & Technology Press, Guangzhou, China, 357pp. (in Chinese).

Ringuet, S., MacKenzie, F.T., 2005. Controls on nutrient and phytoplankton dynamics during normal flow and storm runoff conditions, Southern Kaneohe Bay, Hawaii. Estuaries 28, 327–337.

Sanders, R., Jickellsb, T., Millsc, D., 2001. Nutrients and chlorophyll at two sites in the Thames plume and southern North Sea. Journal of Sea Research 46, 13–28.

Smith, J.W.O., Demaster, D.J., 1996. Phytoplankton biomass and productivity in the Amazon River plume: correlation with seasonal river discharge. Continental Shelf Research 16, 291–319.

Wang, H.L., Huang, B.Q., Hong, H., 1997. Size-fractionated productivity and nutrient dynamics of phytoplankton in subtropical coastal environments. Hydrobiologia 352, 97–106.

Wanninkhof, R., 1992. Relationship between wind speed and gas exchange over the ocean. Journal of Geophysical Research 97, 7373–7382.

Wu, J., Hong, H., Shang, S., Dai, M., Lee, Z., 2007. Variation of phytoplankton absorption coefficients in the northern South China Sea during spring and autumn. Biogeosciences Discussions 4, 1555–1584.

Yin, K., Harrison, P.J., this issue. Nitrogen over enrichment in subtropical Pearl River estuarine coastal waters: Possible causes and consequences. Continental Shelf Research, in press, doi:10.1016/j.csr.2007.07.010.

Yin, K.D., Song, X.X., Sun, J., Wu, M.C.S., 2004. Potential P limitation leads to excess N in the Pearl River estuarine coastal plume. Continental Shelf Research 24, 1895–1907.

Zhai, W.D., Dai, M.H., Cai, W.J., Wang, Y.C., Hong, H.S., 2005a. The partial pressure of carbon dioxide and air–sea fluxes in the northern South China Sea in spring, summer and autumn. Marine Chemistry 96, 87–97.

Zhai, W.D., Dai, M.H., Cai, W.J., Wang, Y.C., Wang, Z.H., 2005b. High partial pressure of CO_2 and its maintaining mechanism in a subtropical estuary: the Pearl River estuary, China. Marine Chemistry 93, 21–32.

Zhang, J., Xu, H., Yu, Z.G., Wu, Y., Li, J.F., 1999. Dissolved aluminum in four Chinese estuaries: evidence of biogeochemical uncoupling of Al with nutrients. Journal of Asian Earth Sciences 17, 333–343.